

## **HYDRAULIC JUMP----THE STATE OF THE ART HYDRODYNAMIC CHARACTERISTICS OF FIXED AND MOVABLE BEDS**

**\*Luoching-Ruey (Edward)**

*Department of Civil Engineering, National Chi-Nan University,  
Nantou, Taiwan*

*\*Author for Correspondence*

### **ABSTRACT**

A hydraulic jump is a phenomenon in the science of hydraulics which is frequently observed in open channel flow such as rivers and spillways with or without sluice gates. When liquid at high velocity discharges into a zone of lower velocity, a rather abrupt rise occurs in the liquid surface of downstream with a distance from the flow inlet. The rapidly flowing liquid is abruptly slowed and increases in height, converting some of the flow's initial kinetic energy into an increase in potential energy, with some energy irreversibly lost through turbulence to heat. In an open channel flow, this manifests as the fast flow rapidly slowing and piling up on top of itself. In this paper, the 2-D analytically hydrodynamic characteristics for submerged hydraulic jump, such as water height, turbulent primary velocity, turbulent shear stress, and turbulent kinetic energy with high Froude number for fixed bed and the primary velocity and the 2-D velocity field for movable bed are solved and then compared with the 2-D width-averaged numerical and experimental results. The comparisons give obviously results for the good applicability of hydraulic jumps.

**Keywords:** *Submerged Hydraulic Jump; Hydrodynamic Characteristics; Turbulent Primary Velocity; Turbulent Shear Stress; Turbulent Kinetic Energy*

### **INTRODUCTION**

In an open channel when water at high velocity discharges into a zone of lower velocity, such as spillway in Figure 1, an abrupt rise on the surface and high turbulence at the bottom in the form of rollers occur (seen Figure 2). The rapidly flowing water is abruptly slowed and increases in height, converting kinetic energy into an increase in potential energy, with some energy irreversibly lost through turbulence. It is one of the important tasks for hydraulic engineers to design a safe and economical energy dissipater. Stilling basins are one of the possible solutions for hydraulic jump to dissipate kinetic energy to produce safe downstream flow, which causes no bed scour and bank erosion. Hydraulic jump was first investigated experimentally (Bidone 1818). Thereafter, many studies were made and the results were quoted by many engineers. But, there is a lack of results on some of the jump characteristics, which may reasonably affect the hydraulic jump phenomenon.

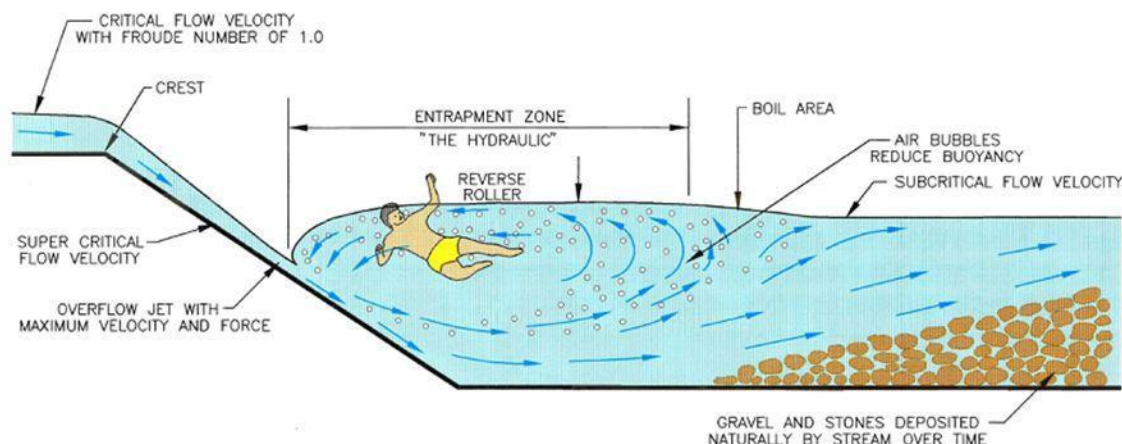


*Hydraulic jump on a dam spillway.*

**Figure 1: The flow of the hydraulic jump on a dam spillway**

## Research Article

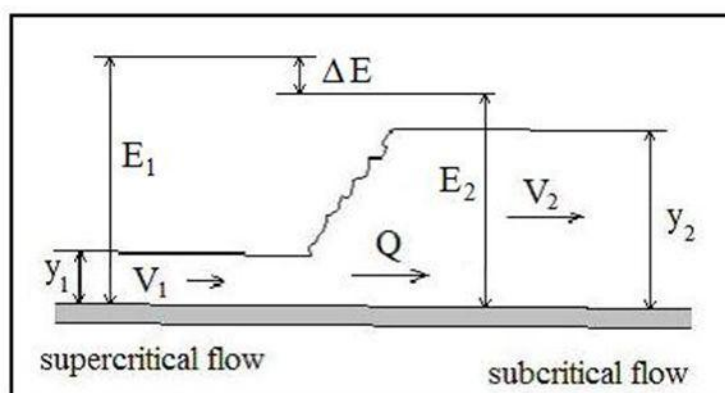
Therefore, their effects need to be explored for a better estimation of safe stilling basin design. The specific force equation has many applications in open channel flow problems. Quantifying of the hydraulic jump phenomenon is an important application of this equation (Figure 3).



Courtesy of Wright Water Engineers, Inc. and ASDSO.

Source: Wright, Kenneth R., Kelly, Jonathan M., Houghtalen, Robert J., & Bonner, Mark R. "Emergency Rescues at Low-Head Dams." Paper presented at Dam Safety 1995, the 12th annual conference of the Association of State Dam Safety Officials, Atlanta, GA, September 1995.

**Figure 2: Turbulent phenomena of hydraulic jump**



**Hydraulic Jump (with Heads and Head Loss)**

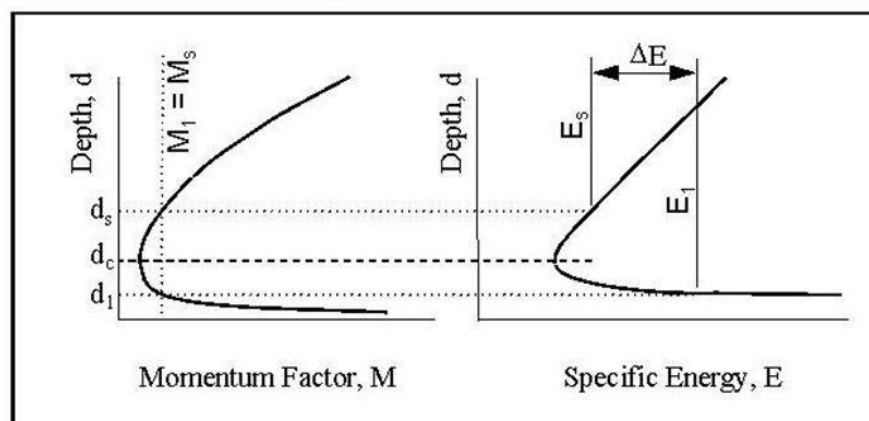


**Figure 3: Specific Momentum and Energy for hydraulic jump**

## Research Article

### Theoretical Considerations of Submerged Hydraulic Jump

Naturally, the channel geometries vary not only in the lateral direction but also in the depth one, or said 3-D, while due to the lack of sufficient data to be used to calibrate this 3-D model, the flow situation may be simplified to 2DV flows with the assumption of quite uniformity in the width direction. The idea of plan turbulent wall jets (Rajaratnam, 1965, 1976), which possessed very strong turbulence, is chosen to describe and derive the primary velocity and turbulent shear stress profiles, which are then used to express the turbulent eddy viscosity. The 2-DV continuity equation and equation of motion are used to derive the secondary velocity and turbulent kinetic energy. Finally, the 2-D  $k-\epsilon$  two-equation model presented by (Rodi, 1980) is used to obtain the energy dissipation rate of the 2-D hydraulic jump flows. The mathematical models of 2DV with width-averaged equations, called VEST, are used for numerical solutions (Luo, 2013). Based on the definitions on Figs. 4, 5, and 6, we summary the analytical solutions (Luo, 2013) as:

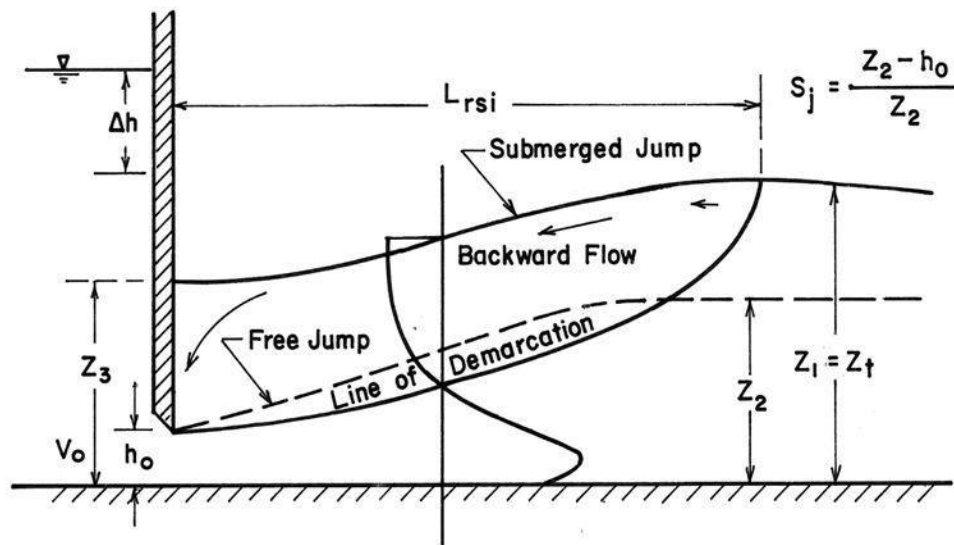


Figure 4: Submerged hydraulic jump (from Rajaratnam, 1965)

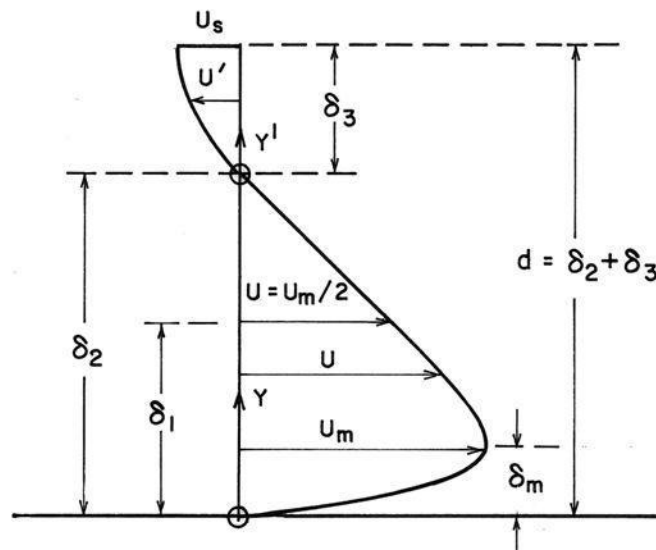
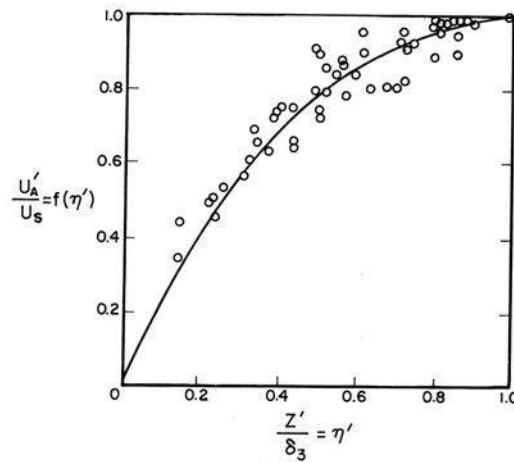


Figure 5: Submerged hydraulic jump (from Rajaratnam, 1965)



**Figure 6: Velocity distribution in the backward flow (from Rajaratnam, 1965)**

**A. Analytical Primary Velocity Profile and Velocity in Depth- Direction**

(a) Forward flow:

$$\frac{U}{U_{\max}} = \exp[-0.905(\eta - 0.125)^2] \quad \dots\dots\dots(1)$$

$$\frac{U_{\max}}{V_0} = 5.395 \left( \frac{x'}{h_0} + 11.2 \right)^{-0.555} \quad \dots\dots\dots(2)$$

$$\frac{\delta}{h_0} = 0.0678 \left( \frac{x'}{h_0} + 11.2 \right) \quad \dots\dots\dots(3)$$

$$x = x_0 + x'$$

$$x_0 = \left( \frac{h_0}{2} \right) \cot \theta$$

$$\theta = 1.94^\circ \quad \dots\dots\dots(4)$$

$$z_c = \sqrt[3]{\frac{(V_0 h_0)^2}{g}}; \quad F_{r0} = \frac{V_0}{\sqrt{g h_0}} \quad \dots\dots\dots(5)$$

where Z2 is the subcritical sequent depth without submerged hydraulic jump happening.

(b) Backward flow:

$$\frac{U'}{U_s} = f(\eta') = -1.122 (\eta')^2 + 2.098 \eta' \quad \dots\dots\dots(6)$$

$$\frac{U_s}{V_0} = -0.27 \sin(\pi \alpha) \quad \dots\dots\dots(7)$$

where  $\eta$ =dimensionless boundary layer displacement= $z/\Delta$ ;  $2.0 \leq \eta \leq 2.5$ , and with  $\eta'=z'/\delta_3$ , and  $\delta_3= h-2.5\delta$ , the velocity distribution in the backward flow, and  $U_s$  is the surface velocity of adverse flow. The velocity profile of in vertical direction is expressed as:

## Research Article

$$\begin{aligned}
 W = & \left( \frac{0.017\delta V_0}{h_0} \right) \left( \frac{x'}{h_0} + 11.2 \right)^{-1.665} \operatorname{erf} \left[ 0.951 \left( \frac{z}{\delta} - 0.125 \right) \right] + 0.66 V_0 \cdot \\
 & \left( \frac{x'}{h_0} + 11.2 \right)^{-0.555} \left[ \frac{0.34z^3}{\delta^3} + \frac{0.244z^4}{\delta^4} - \frac{z^2}{16\delta^2} - \frac{0.181z^5}{\delta^5} \right] + \\
 & + 0.27 V_0 \sin(\pi \alpha) \left[ \frac{0.18z^2}{\delta_3} - \frac{0.13z^3}{\delta_3^3} \right] - 0.27 V_0 \operatorname{erf} \left[ \frac{1.25z}{h} - 0.12 \right] + \\
 & - 0.17 V_0 \left[ \frac{0.77z^3}{h_0^3} + \frac{0.73z^4}{h_0^4} - \frac{0.71z^5}{h_0^5} - \frac{0.11z^2}{h_0^2} \right] - 0.27 V_0 \sin(\pi \alpha) \cdot \\
 & \left[ \frac{0.18z^2}{(h - 1.9h_0)^2} - \frac{0.13z^3}{(h - 1.9h_0)^3} \right]
 \end{aligned} \tag{8}$$

where

$$\frac{z}{h_0} = \frac{z_3}{h_0} + \left( \frac{1.48 L_{rsj}}{h_0} \right) \ln [\csc(\pi \alpha) - \cot(\pi \alpha)] \tag{9}$$

### B. Analytical Turbulent Shear Stress

$$\overline{\tau_{xz}} = \rho \bar{v}_t \left( \frac{\partial U}{\partial z} \right) \tag{10}$$

$$\begin{aligned}
 v_{tz} = & \frac{u_*^2 \left( 1 - \frac{z}{h} \right)}{\left( \frac{dU_1}{dz} + \frac{dU_2}{dz} \right)} = \frac{(\tau_{xz}/\rho)}{(\partial U/\partial z)} \\
 = & \delta^4 \left( \frac{x'}{h_0} + 11.2 \right)^{0.555} \left[ \frac{u_*^2 (h + 0.37\delta)}{9.3z^3 h V_0} - \frac{u_*^2}{9.3z^2 h V_0} \right]
 \end{aligned} \tag{11}$$

where  $U_1$  the forward flow velocity in Eq. (1), while  $U_2$  in Eq. (6)

### C. Analytical Turbulent Kinetic Energy and Turbulent Energy Dissipation Rate

$$\begin{aligned}
 \bar{k} = & \frac{1}{2} \left\{ 0.6 h_0 V_0^2 \left( \frac{vh}{RV_0 h_0} \right)^{1/4} \left[ \left( \frac{2.95}{h_0} \right) \bar{P}_*^{0.334} + \left( \frac{1.5}{h_0} - \frac{6Z}{hh_0} \right) \bar{P}_*^{-0.666} + \right. \right. \\
 & \left. \left( \frac{30Z}{h_0^2} - \frac{101Z}{h_0^2} - \frac{118Z^2}{hh_0^2} \right) \bar{P}_*^{-1.666} + \left( \frac{542Z^2}{h_0^3} \right) \bar{P}_*^{-2.666} + \right. \\
 & \left. \left. - \left( \frac{11596Z^3}{h_0^4} \right) \bar{P}_*^{-3.666} + \left( \frac{93224Z^4}{h_0^5} \right) \bar{P}_*^{-4.666} \right] - U^2 \right\}
 \end{aligned} \tag{12}$$

where



## Research Article

$$P_* = \left( \frac{X}{h_0} + 11.2 \right)$$

$$\bar{\varepsilon} = C_\mu \left( \frac{\bar{k}^2}{v_t} \right) \dots \dots \dots (13)$$

### Comparisons

According to the Froude number of inflow, the hydraulic jump can be denoted into 4 cases as the following: the pre-jump stage for Froude number is between 1.7 and 2.5; the transition stage for Froude number between 2.5 and 4.5; the well-balanced jump for Froude number between 4.5 and 9.0; and the effective jump but rough surface downstream for Froude number great than 9.0 (see Figure 7). The comparisons are separated into two groups: the one is for fixed bed situation, and the other is presented for the movable bed cases.

#### A. For Fixed Bed

The following results will show us the comparisons between analytical solutions of this study and the ones of numerical and/or experimental solutions (Long, 1991) for fixed bed situations, including water depth with different Froude number and varied  $S_j$  in Figure 8, primary velocity profile in Figure 9, turbulent shear stress in Figure 10, and turbulent kinetic energy in Figure 11.

#### B. For Movable Bed

And the comparisons for movable bed are also given:

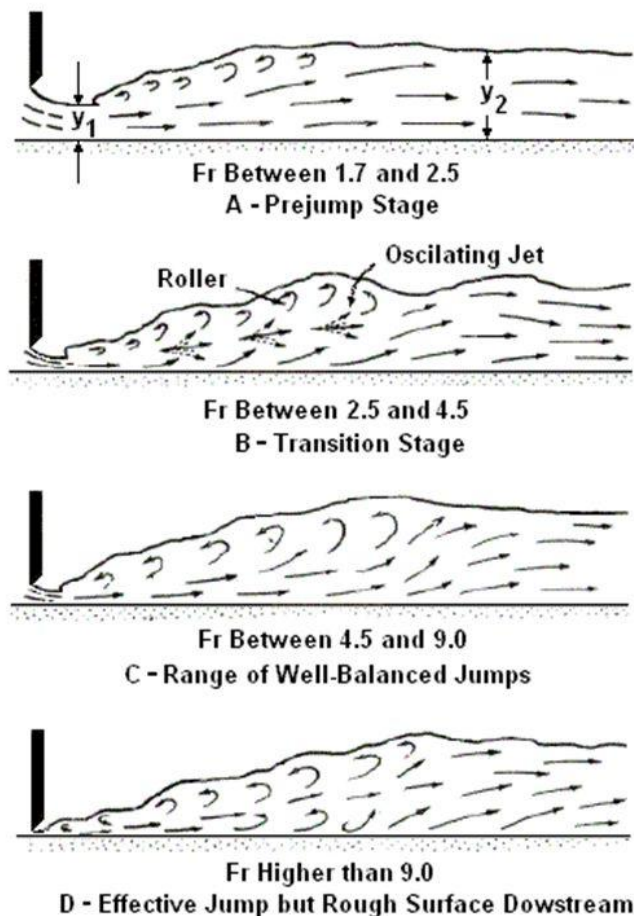


**Figure 7: The classifications of hydraulic jumps based on the Froude numbers**

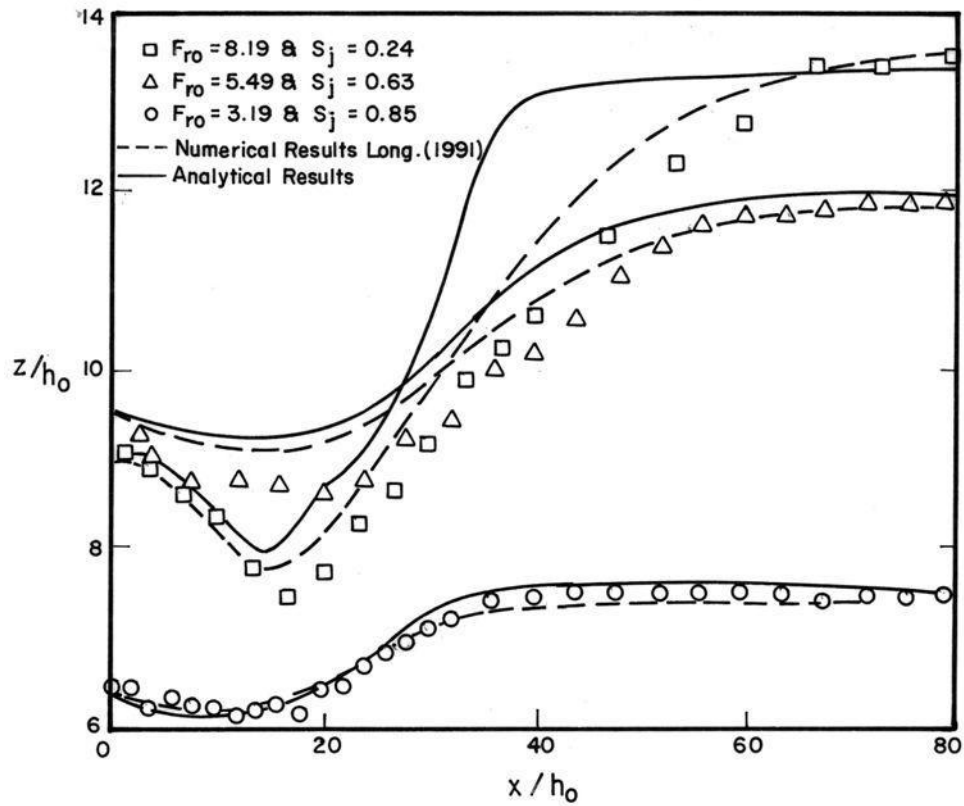


**Figure 8: Comparison of water surface profiles among the analytical, experimental, and numerical results for supercritical open channel flows of submerged hydraulic jumps**

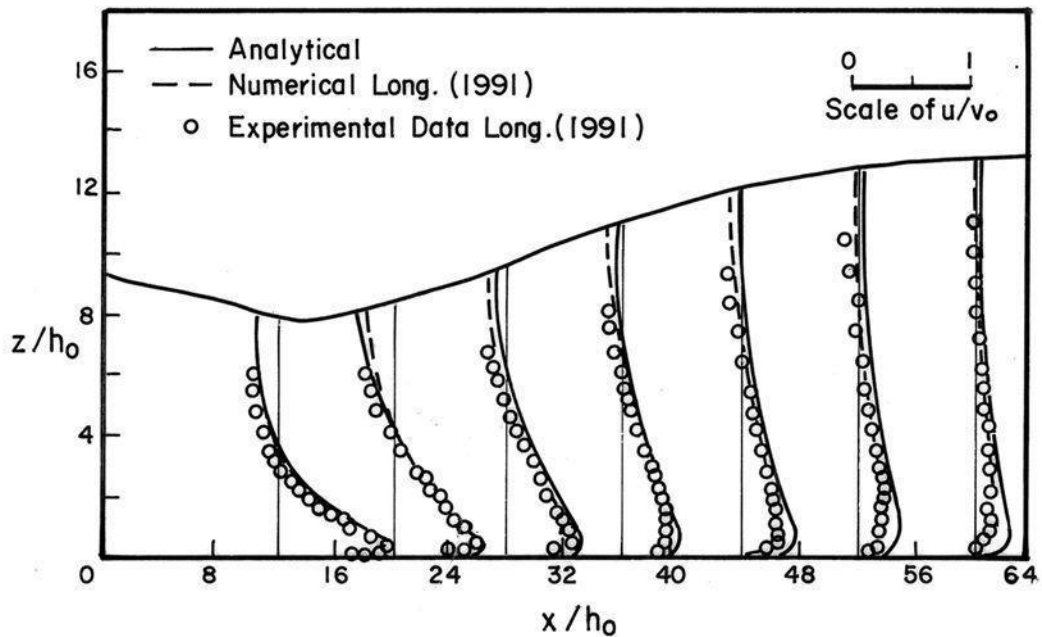


**Figure 9: Comparisons of primary velocity profiles among the analytical, experimental, and numerical results for supercritical open channel submerged hydraulic jumps for  $F_{ro}=8.19$  and  $S_j=0.24$**

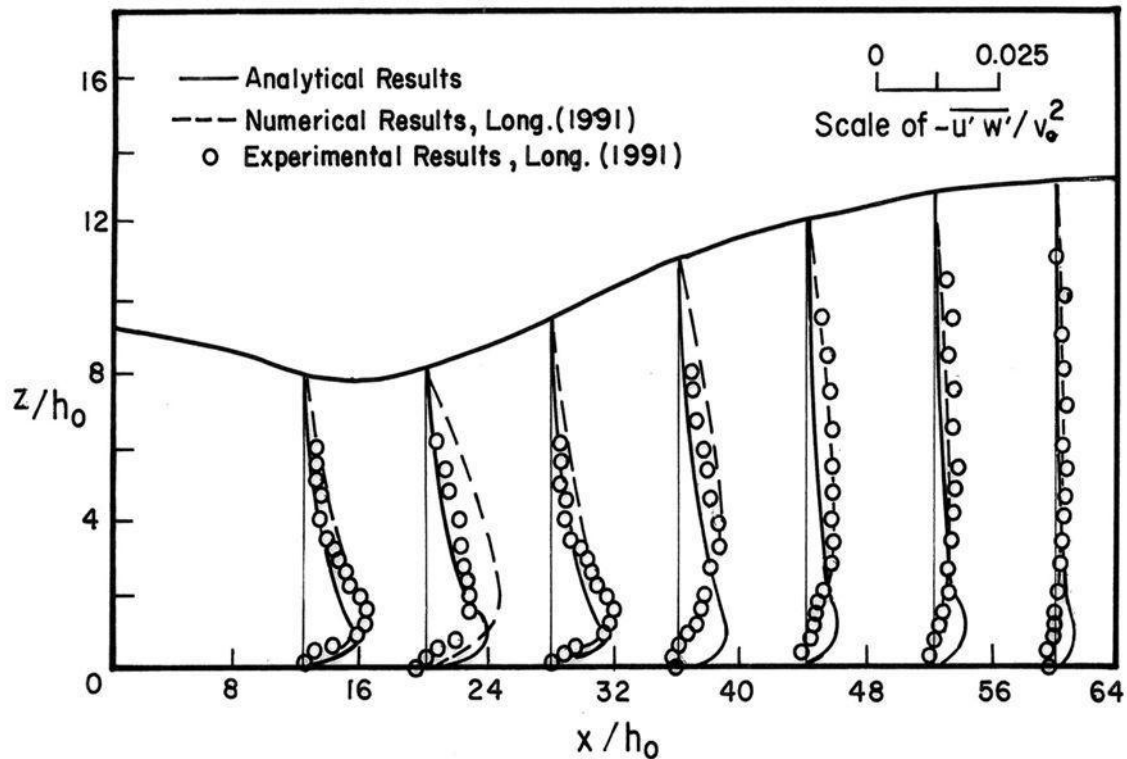


**Figure 10: Comparisons of turbulent shear stress distribution among the analytical, experimental, and numerical results for supercritical open channel submerged hydraulic jumps for  $Fro=8.19$  and  $Sj=0.24$**

With the consideration of the erodible bed situation, the functions of the laws of the wall and the wake are combined as the following equation,

$$\frac{U}{u_*} = \frac{1}{\kappa} \ln \left( \frac{zu_*}{v} \right) + C + \frac{T_0}{\kappa} \omega \left( \frac{z}{\delta} \right) \quad (14)$$

where  $T_0$  is the initial value of shape factor without adverse pressure gradient;  $\kappa=0.40$ ;  $C=0.49$ ; and  $\omega(z/\delta)$  is called the law of the wake with the form of

$$\omega \left( \frac{z}{\delta} \right) = \omega(\xi) = -4.7468\xi^3 + 7.1397\xi^2 - 0.3869\xi \quad (15)$$

where  $\xi=0$ ,  $\omega(\xi)=0$ , and  $\xi=1$  with  $\omega(\xi)=2.0$ . From Eq. If the length of the apron is longer than the one of the hydraulic jump, then the standard logarithmic velocity profile happens within the region of apron and the foundation at the end of the apron is not necessary too deep. But when the apron is not long enough, the submerged hydraulic jump still happens on the surface of erodible bed, then due to the stronger turbulence within the region of submerged hydraulic jump, the movable bed is eroded, and thus foundation is constructed very deep. The development of the internal layer,  $\delta_{i1}$ , if  $\delta_{i0}$  is the boundary layer calculated by Eq. (3) at the end of the rigid bed, then when  $\delta_{i1}=10\delta_{i0}$ , the two boundary layers will meet together. The velocity profiles of Eqs. (1) and (7) will be still used here by only changing  $\delta_1$  and  $\delta_3$  into  $\delta_t$  and  $\delta_{t3}$  and adding  $\delta_t$  in the erodible bed in Figures 12 and 13, where  $\eta_t = -(z/\delta_t)$ , and the boundary conditions

$$\eta_t = -0.72, U/U_{max} = 0.5; \text{ and } \eta_t = 2.00, U/U_{max} = 0.0; \quad (16)$$



## Research Article

Here,  $\eta$  in Eq. (1) is modified into  $\eta_t$  to be used.

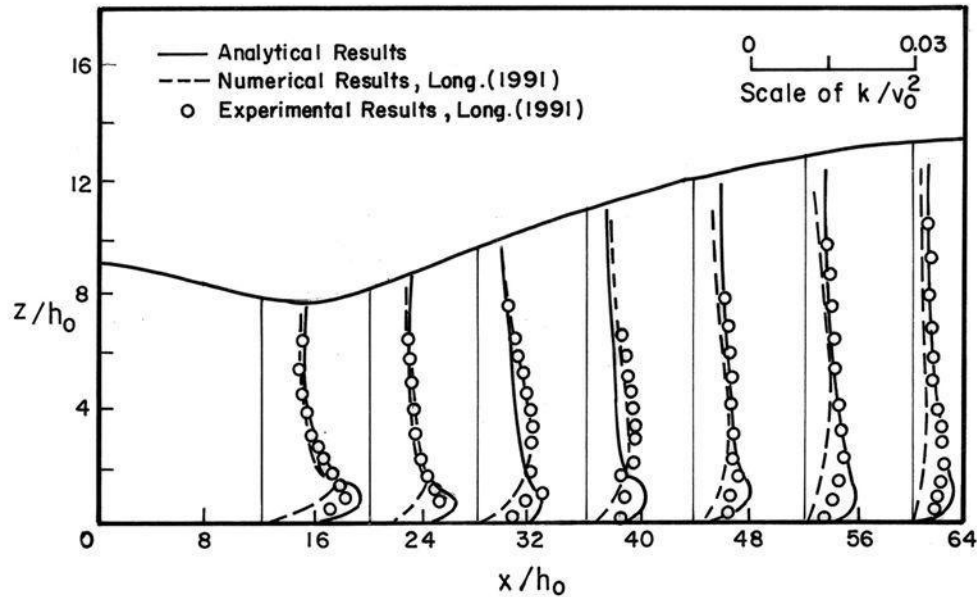


**Figure 11: Comparisons of turbulent kinetic energy distribution among the analytical, experimental, and numerical results for supercritical open channel submerged hydraulic jumps for  $Fro=8.19$  and  $Sj=0.24$**

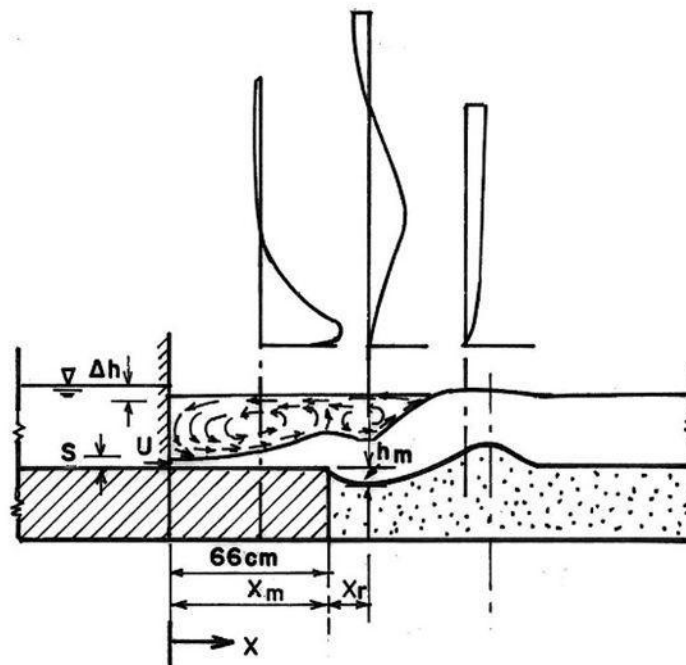


**Figure 12: Diffused jet along with typical velocity profile**

The comparisons among the analytical and the ones of numerical and/or experimental solutions (Tran, 1991) for fixed bed for the scoured bed situation are expressed in Figures 14 and 15. In Figure 14, the greater velocity field from the analytical results than the one from experimental or numerical results. There are 3 eddy zones existing in the scoured bed in figures, the acceleration velocity profile are used to

## Research Article

predict the velocity distribution along the front inclined dune surface while good prediction by using deceleration velocity profiles along the back inclined velocity profiles along the back inclined surface of dunes.

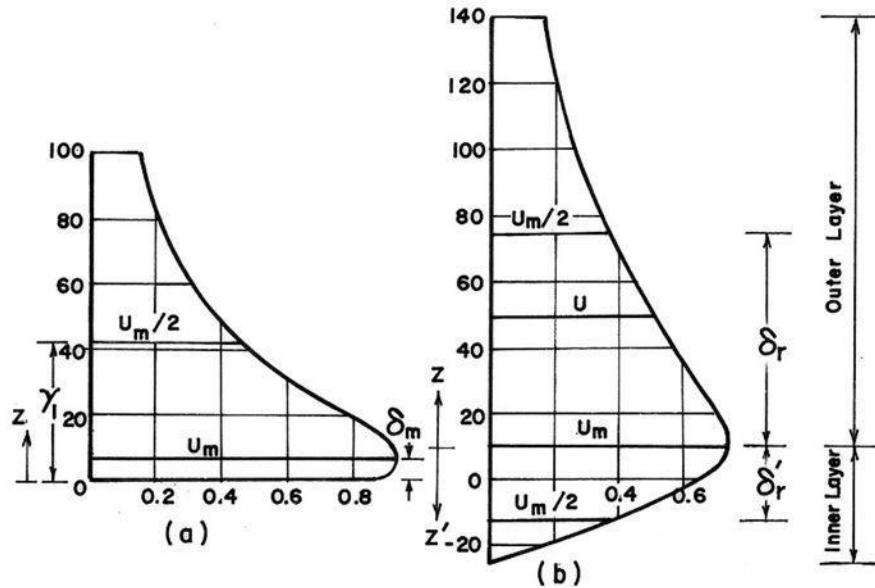


Figure 13: Typical mean velocity profiles: (a) rigid apron; (b) scoured hole

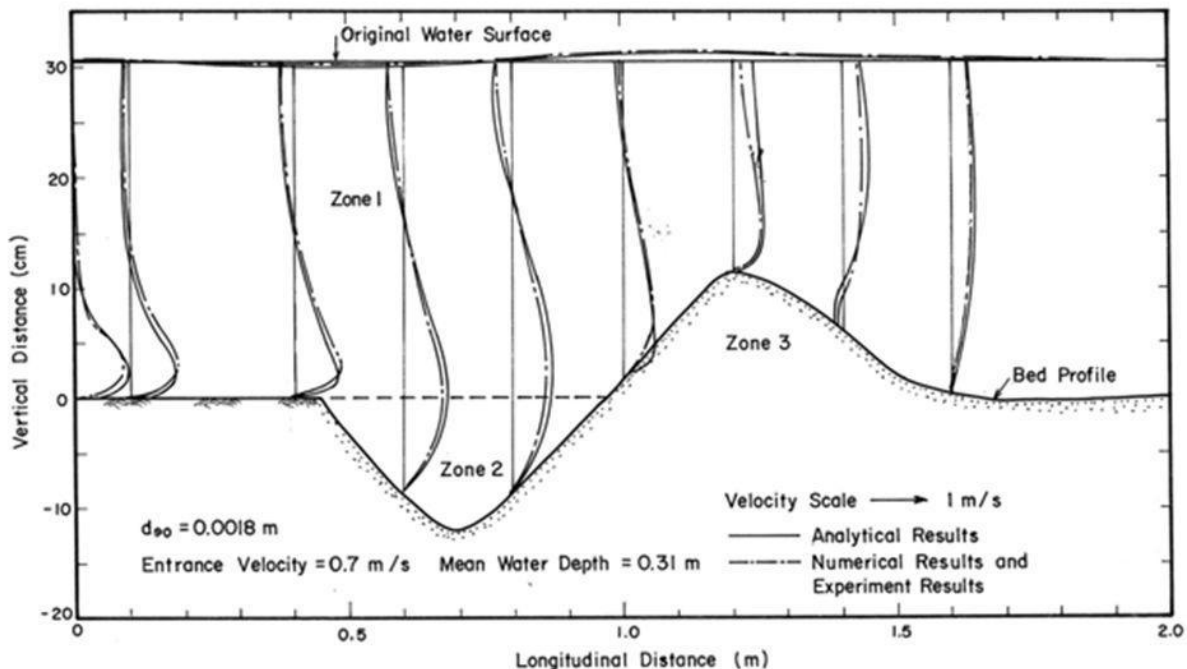


Figure 14: Comparisons of 2DV velocity component along primary flow direction, X, among analytical, numerical (2D-VEST) and experimental results with sluice gate and scoured bed

## Discussion and Conclusions

In Figs. 8, 9, 10 and 11, the analytical results give obviously good agreements with the ones of numerical model and experiments, even the analytical results give a little larger values. There are three eddy zones in Figs. 14 and

## Research Article

15. The torque due to the forward and the backward velocities is formed in zone 1. Because of the existence of scoured hole, the eddy happens in zone 2. The adverse pressure gradient due to deceleration velocity profiles cause the third and smaller eddy in zone 3.

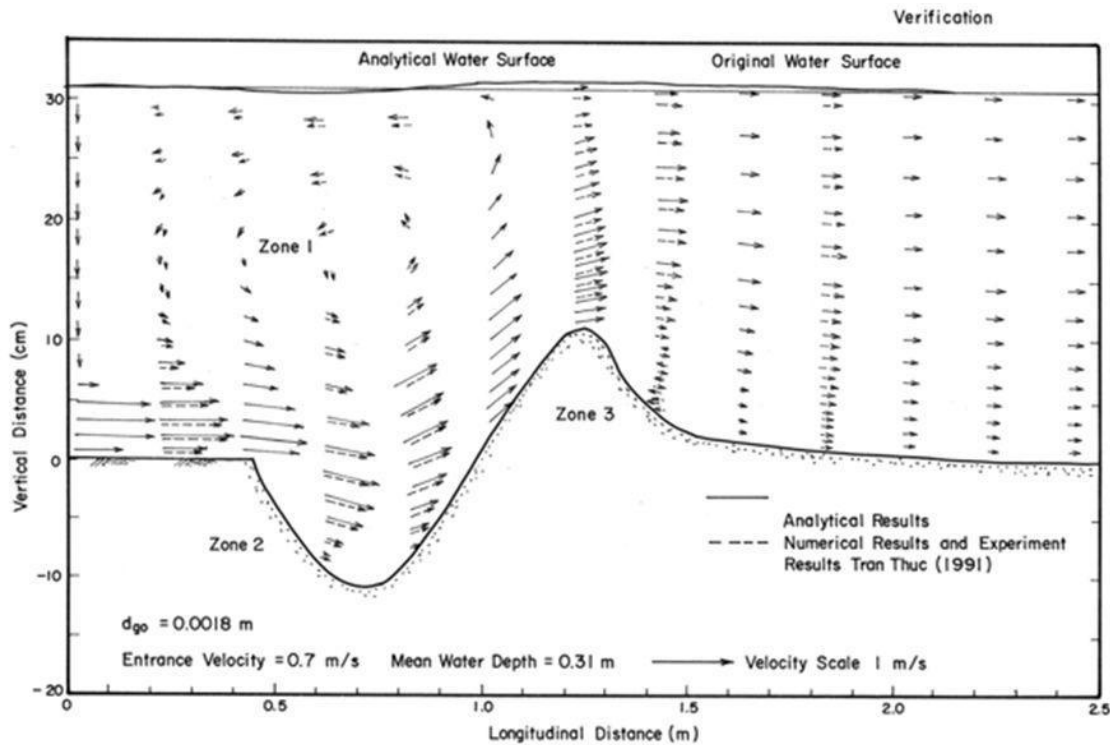


**Figure 15: Comparisons of 2DV velocity vector field among analytical, numerical (2D-VEST) and experimental results with sluice gate and scoured bed**

In this study, the analytical turbulent velocities, turbulent viscosity, turbulent shear stress, turbulent kinetic energy, and energy dissipation rate for submerged hydraulic jumps with sluice gate and with the rigid or the erodible bed are derived. The very good predictions for the case of submerged hydraulic jumps on the primary velocity, water levels, turbulent shear stresses, and turbulent kinetic energy are presented after the comparisons with numerical and experimental results even the analytical results have a little larger values than the ones from others. These hint that when you utilize the numerical model for the case of submerged hydraulic jump of higher Froude number inflows with sluice gate, it is necessary to modify the magnitudes of the standard parameter in the  $k-\epsilon$  equations.

## REFERENCES

- Bidone Giorgio (1881).** *Observations on the Height of Hydraulic Jump*, report presented in Royal academy of sciences of Turin 21–80.
- Long D, Steffler PM and Rajaratnam M (1991).** A Numerical Study of Submerged Hydraulic Jumps. *Journal of Hydraulic Research, IAHR* 29(3) 56-66.
- Luo CR (2013).** Analysis and Application of Hydraulic Jump. *International Journal of Engineering and Innovation Technology (IJEIT)* 3(2) 519-524.
- Rajaratnam N (1965).** Submerged Hydraulic Jump. *Journal of Hydraulic Engineering, ASCE* 104(3).
- Rajaratnam N (1976).** *Turbulent Jets* (Elsevier Scientific Publishing Company) Amsterdam-Oxford-New York.
- Rodi W (1980).** *Turbulence Models and Their Application*.
- Tran Thuc (1991).** Two-Dimensional Morphological Computations Near Hydraulic Structures, Dissertation No. WA-91-2, Asian Institute of Technology, Bangkok, Thailand.